CONF-801040--2

LA-UR -80-2952

TITLE: DIAGNOSTICS AND PERFORMANCE EVALUATION OF MULTIKILOHERTZ CAPACITORS

MASTER

AUTHOR(S): G. McDuff, W. C. Nunnally, K. Rust, and J. Sarjeant

SUBMITTED TO: Special Symposium on High Energy Density Capacitors and Dielectric Materials
1980 CEIDP Conference, October 28, 1980
Boston, Massachusetts

University of California

LOS ALAMOS SCIENTIFIC LABORATORY
Post Office Box 1663 Los Alamos, New Mexico 87545
An Affirmative Action/Equal Opportunity Employer

Form No. 836 R1
St. No. 2629
12/78

UNITED STATES
DEPARTMENT OF ENERGY
CONTRACT W-7405-ENG. 36

DIAGNOSTICS AND PERFORMANCE EVALUATION OF MULTIKILOHERTZ CAPACITORS*

G. McDuff, W. C. Nunnally, K. Rust, and J. Sarjeant
Los Alamos Scientific Laboratory
Los Alamos, New Mexico 87545

ABSTRACT

The observed performance of nanofarad polypropylene-silicone oil, mica paper, and polytetrafluoroethylene-silicone oil capacitors discharged in a 100-ns, 1-kA pulse with a pulse repetition frequency of 1 kHz is presented. The test facility circuit, diagnostic parameters, and the preliminary test schedule are also discussed. In addition, the basic capacitor construction details are outlined as a basis for discussion of the observed failure locations and proposed failure mechanisms. Most of the test data and discussion presented involves the polypropylene-silicone oil units.

I. INTRODUCTION

A. Program Purpose

The development of long-life, multikilohertz, fast-discharge capacitors is essential to many future high-energy applications including nonnuclear or directed energy weapons, isotope separation lasers, short-pulse radar modulators, and electronic warfare and countermeasure pulse generators. The development program discussed in this paper is in support of the Los Alamos Scientific Laboratory (LASL) Molecular Laser Isotope Separation (MLIS) Program. The primary purposes of this program are:

- To determine qualitative capacitor dielectric system behavior in a short-pulse multikilohertz repetition rate, high di/dt discharge environment.
- To understand, model, and eliminate the failure mechanisms that are observed in the above environment.
- To develop, in conjunction with capacitor manufacturers, long-life, reliable capacitors for use in the high di/dt, multikilohertz laser systems required for MLIS.

*This work was performed under the auspices of the US Department of Energy.

B. Program Rationale

The program rationale is to evaluate capacitor technology provided by industry to determine and understand the failure mechanisms and to work with the manufacturers to provide better units. This is in contrast to a basic research program to develop new dielectrics and impregnants. Rather, this program seeks to determine the capacitor system weak points, the characteristic failure mechanisms, and the required dielectric characteristics compatible with multikilohertz, high di/dt discharges. This program should provide direction to future basic dielectric system research and development. A natural result of this program is the determination of the operating limits of present capacitor technology in different capacitor structures.

II. TEST FACILITY

A. Discharge System

The requirements of the capacitor discharge test circuit are determined by the capacitor test criteria listed in Table I.

TABLE I
CAPACITOR TEST PARAMETER RANGES

Parameter	Value	Unit
Capacitance	0.5-2	nF
Voltage	10-100	kV
Discharge time	60-100	ns
Reversal	10-15	%
Pulse repetition frequency	0.1-5	kHz
Peak current	0.1-5	kA
Life	10^8-10^{10}	discharges

A simplified circuit diagram of the capacitor discharge loop is shown in Fig. 1. Figure 1 also illustrates the thyratron switch used to discharge several capacitors in parallel through individual load resistors and

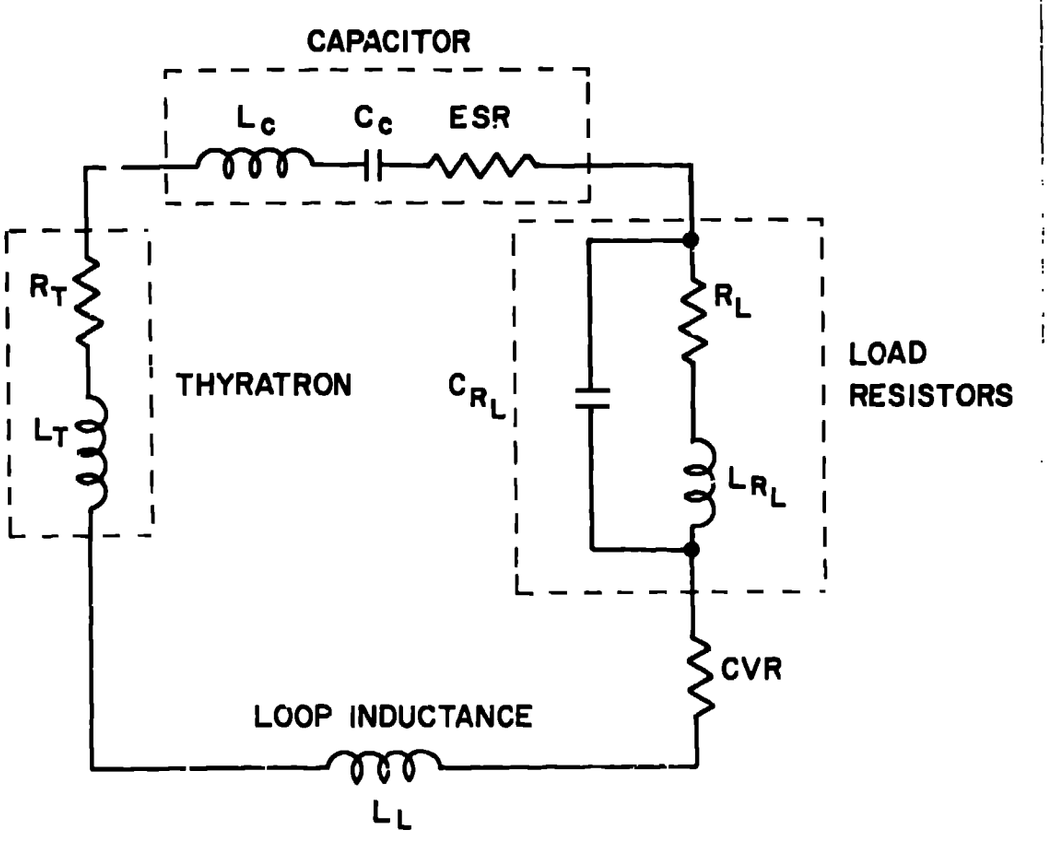

Fig. 1. Capacitor Discharge Circuit

the current viewing resistors (CVR) used to monitor the individual capacitor-load currents and the total current through the thyratron.

B. Charge Systems

The capacitor under test (CUT) can be charged using either resonant or transformer pulse charging. The characteristics of the two charge methods are listed in Table II.

TABLE II

CAPACITOR CHARGE SYSTEM PARAMETERS

Parameter	Value	Unit
I. Resonant Charge System		
Voltage maximum	1-60	kV
Charge time	0.5-2	ms
Capacitance value	1-5	nF
Maximum average power	20	kW
Repetition frequency	0.1-5	kHz
II. Pulse Transformer Charge System		
Voltage maximum	1-70	kV
Charge time	0.75-1.7	μs
Capacitance value	1-5	nF
Maximum average power	50	kW
Repetition frequency	0.1-5	kHz

The resonant charge circuit is shown in Fig. 2 and illustrates several design features of the system as a whole. First, the trigger link is fiber optic coupled and has less than 0.5-ns total jitter. Also the necessity of snubber and transient filter networks in the charge system is evident.

C. Shielding

Extensive care in planning the grounding and shielding system for the development facility was necessary to measure nanosecond transients with millivolt resolution. With the basic shielding layout and design shown in Fig. 3, the facility has been operated at an average power level of 50 kW and repetition rates of 2 kHz without electromagnetic interference problems.

D. Diagnostics

The heart of the test facility diagnostic system is a Tektronix transient digitizer word processor. Using Tektronix 7912 transient waveform

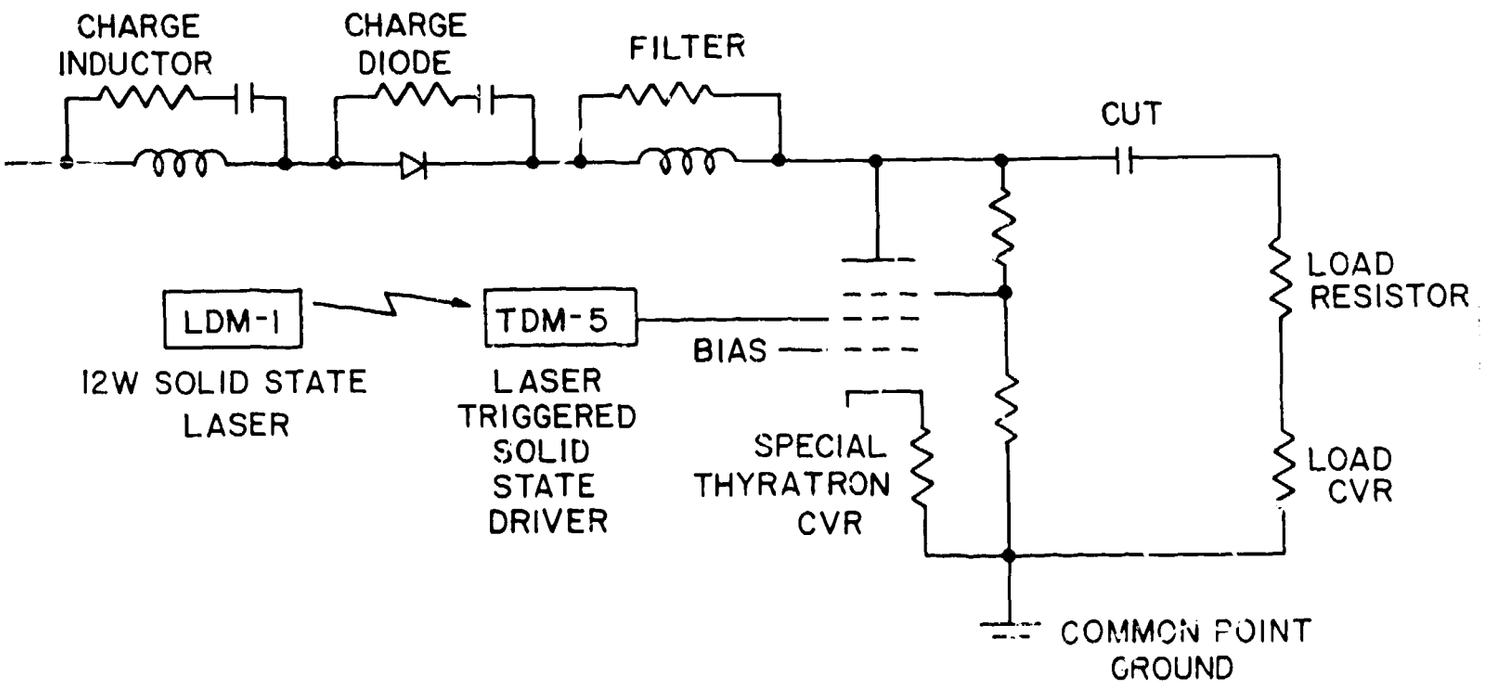

Fig. 2. Resonant charge circuit.

digitizers, each of five capacitor currents and voltages can be measured and recorded sequentially by the data-acquisition system. A 100-kV voltage probe with a frequency response from 0-300 MHz has been developed for measuring the circuit voltages. Nanosecond response from the current probes (CVRs) and voltage probes is required to monitor corona fluctuations in real time during the charge and discharge of the capacitor under test. The basic parameters for the facility diagnostic system are listed in Table III.

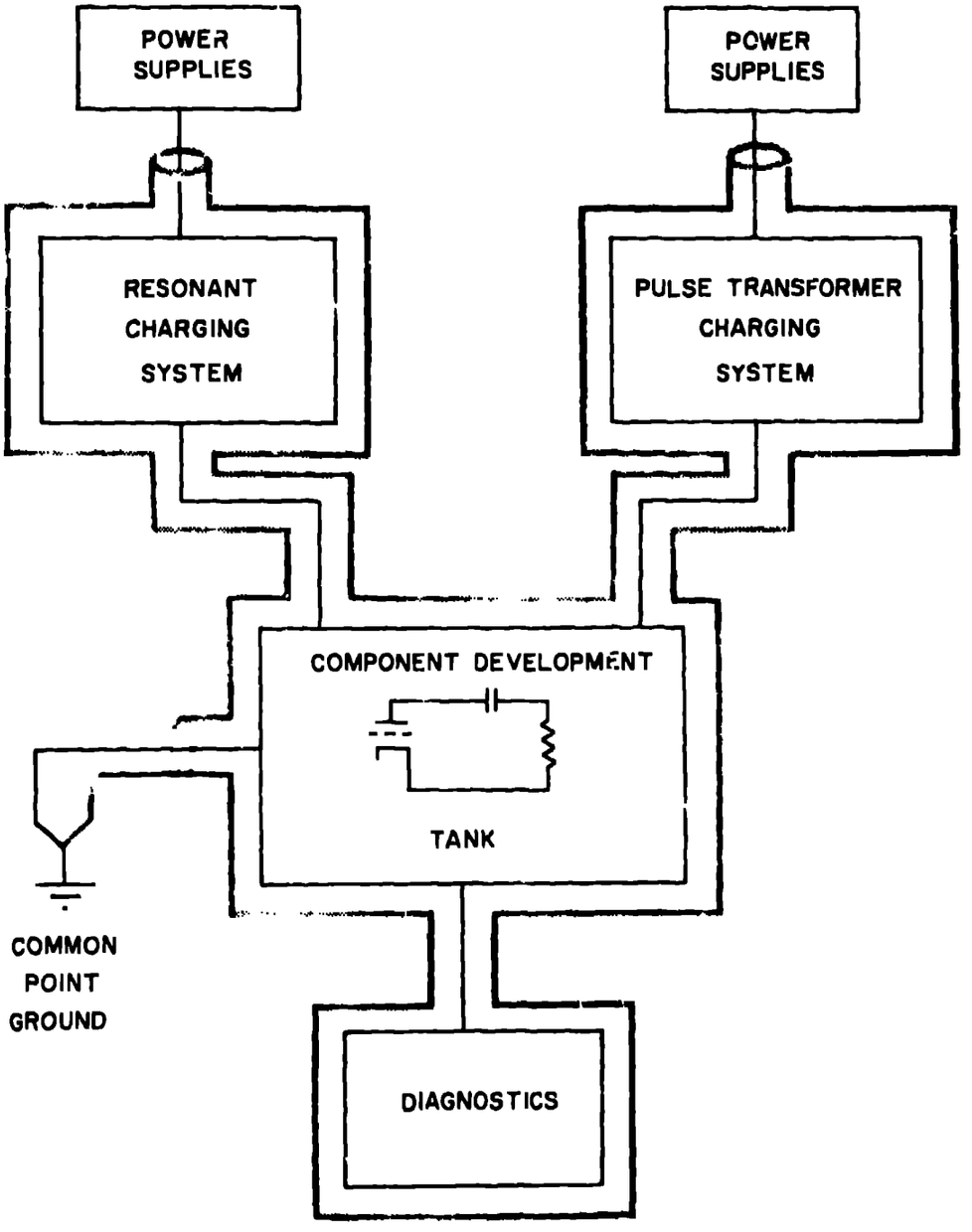

Fig. 3. Facility grounding and shielding system.

TABLE III

CAPACITOR TEST FACILITY DIAGNOSTIC PARAMETERS

Diagnostic	Parameter	Value	Unit
Voltage Probe	Voltage range	0-100	kV
	Attentuation factor	2000	
	Input impedance		
	ac surge ($t < 5$ ns)	1000	Ω
	dc	1000M	Ω
	Frequency response	0-250	MHz
	Amplitude error	±2.5	%
Current Viewing Resistor	Current range	0.005-50	kA
	Attenuation factor	$1\text{-}10^{+4}$	
	Insertion impedance	$1\text{-}10^{-4}$	
	Frequency response	0-500	MHz
	Amplitude error	±2	%
Change di/dt Probe	Frequency response	0-500	MHz
	Amplitude error	±2	%
Overall System Response	Accuracy	±4	%
	Frequency response	0-500	MHz

The data-handling capability of the Tektronix data-acquisition system allows calculation of the following parameters during discharge:

Circuit component impedance

Component power flow

Energy flow

Equivalent series resistance of resistor

The resolution of the diagnostic system is such that a change in circuit parameter values of 0.5% can be detected.

III. PRELIMINARY CAPACITOR EVALUATION

Three types of capacitors have been evaluated:

- Reconstituted mica paper
- Polytetrafluoroethylene (PTFE) impregnated with silicone oil
- Polypropylene impregnated with silicone oil

The test sequence begins with a preliminary life test of the capacitor at a peak discharge current of 1 kA in a near critically damped 100-ns wide pulse and a discharge pulse repetition frequency (PRF) of 1000 Hz. During the preliminary tests, the capacitor stud or tab temperature is monitored and life data are recorded up to 10^8 shots. Both the mica and the PTFE capacitors operated for greater than 10^8 shots without failure. The polypropylene capacitors failed at approximately 3×10^6 discharges. The temperature rise observed on the capacitor terminals was negligible for the three types of capacitors tested.

The possible energy density of polypropylene-silicone oil (PPSO) capacitors is higher than mica and PFTE units because of the higher dielectric strength. The PPSO capacitors were chosen for further investigation because of the energy density potential, availability, and low cost of polypropylene units, and the assumption that the failure mechanisms observed would occur in the other units but at much longer lifetimes. In order to discuss the failure mechanisms observed, a description of the capacitor geometry and fabrication methods is required.

IV. CAPACITOR CONSTRUCTION

The basic capacitor section used in the PPSO and PFTE units is shown in Fig. 4. The capacitor sections are spirally wound into capacitor packs shown in Fig. 5. The packs are then soldered to successive packs and terminals shown in Fig. 6. The capacitor packs of the initial units tested were connected through compression only. This method proved unsatisfactory for the intended service because of arcing observed between packs during discharge due to poor contact. Subsequent capacitor packs were soldered in series as indicated in Fig. 5. The 50-kV capacitors have 10 series packs, 30-kV capacitors have 6 series packs. This is a dc voltage of 5 kV per capacitor pack, which has one active region and two margins. The PPSO average dielectric system stress is 1250 V/mil at rated voltage. The

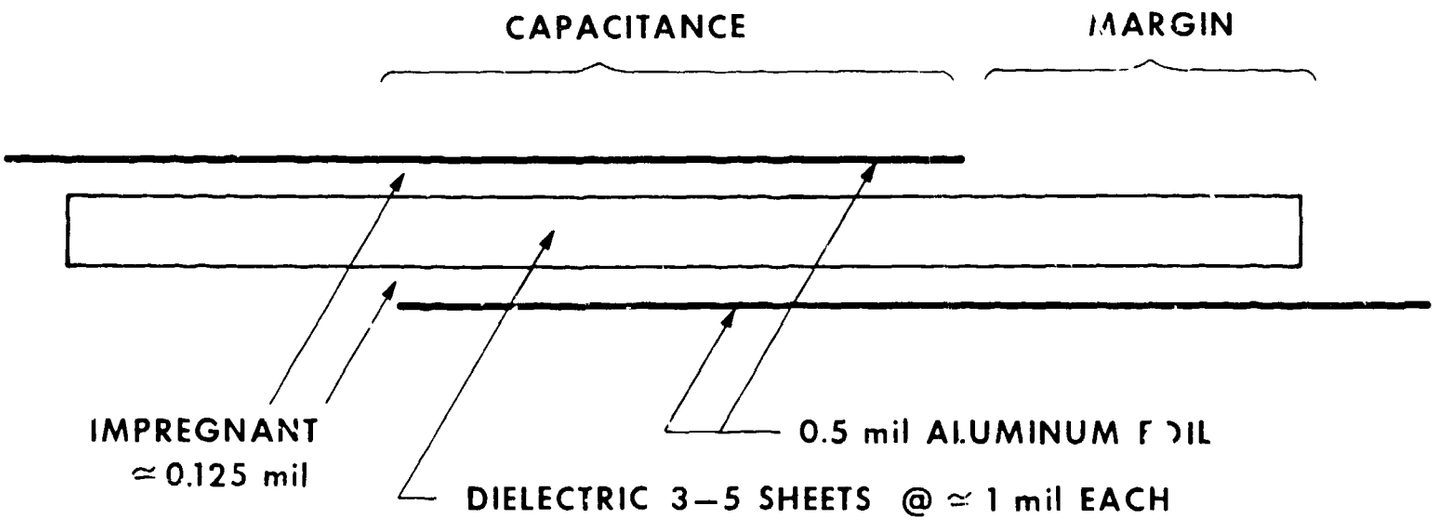

Fig. 4. Basic capacitor section.

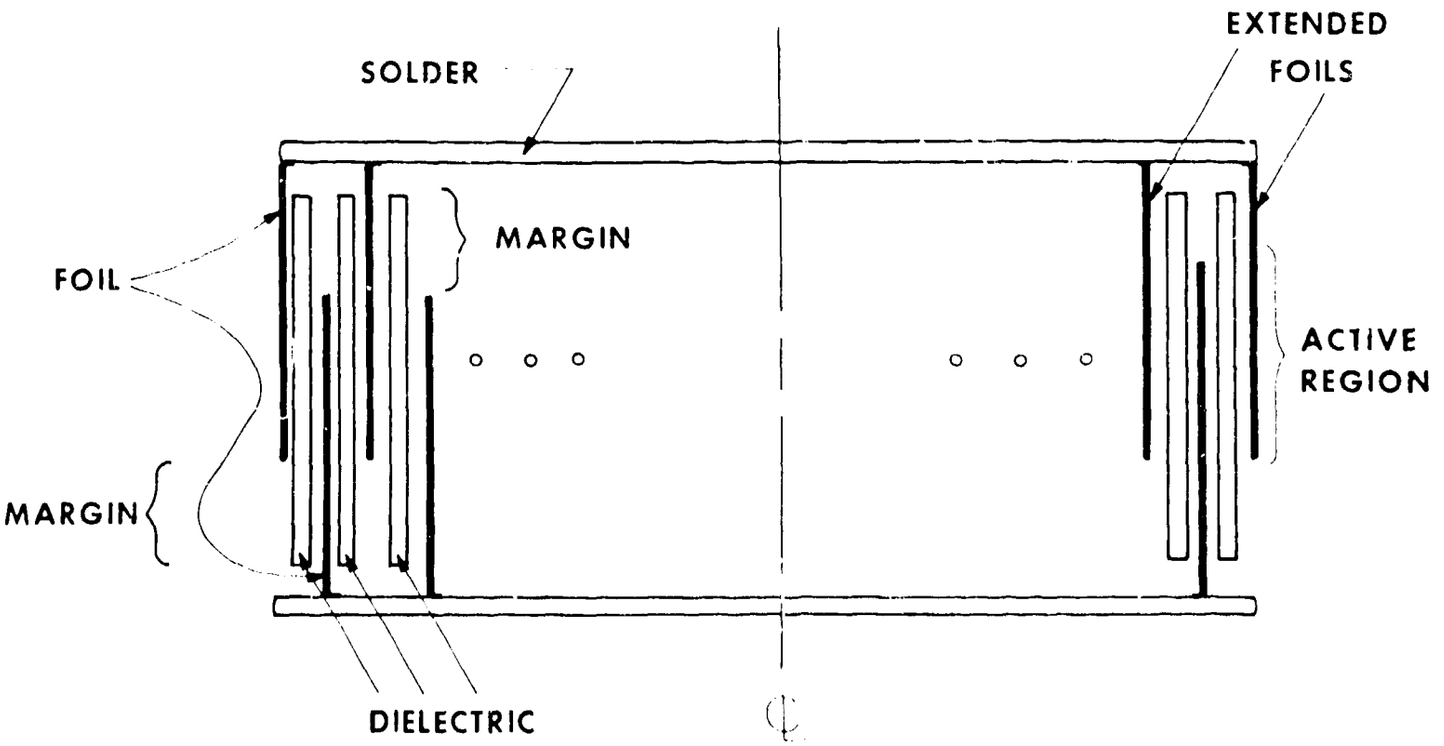

Fig. 5. Basic capacitor pack.

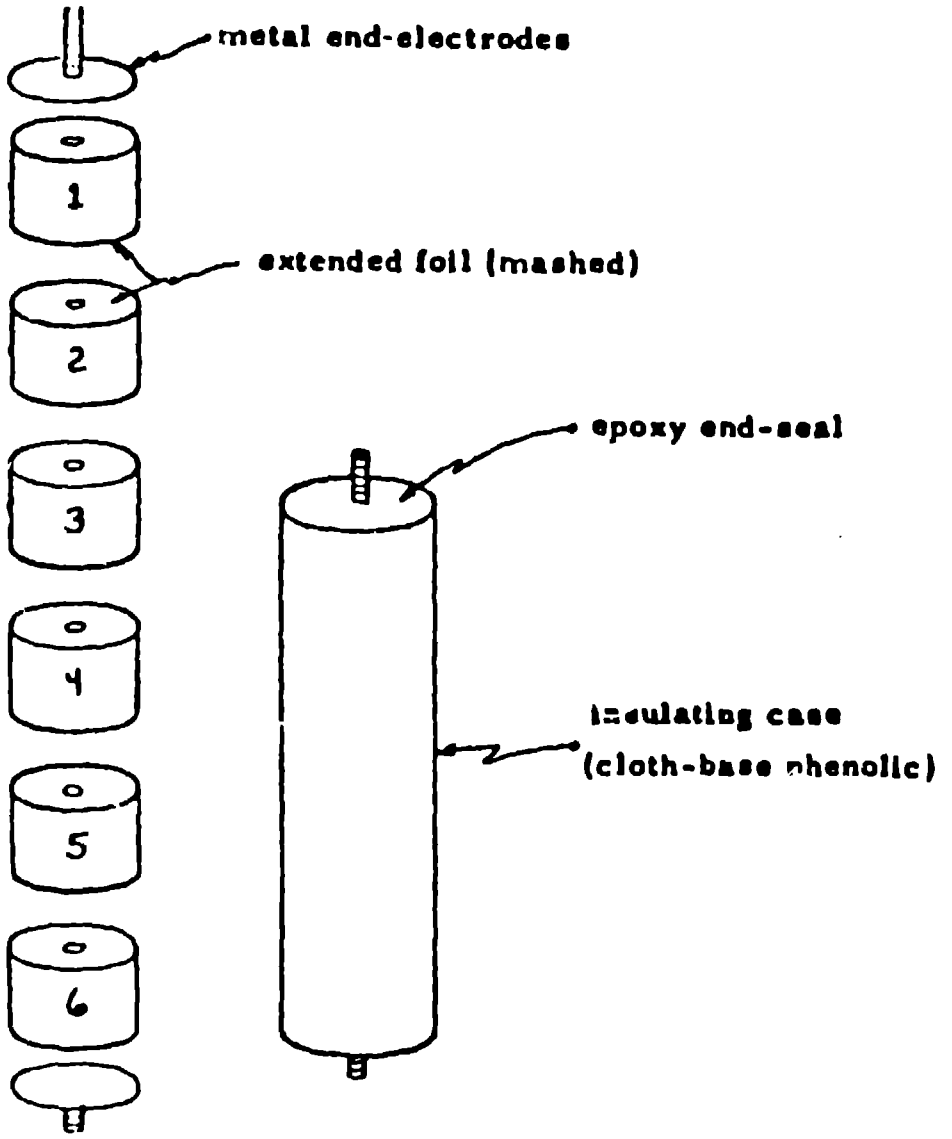

Fig. 6. Capacitor fabrication.

capacitor packs are enclosed in a phenolic tube and then vacuum impregnated with silicone oil. The PPSO units tested used a total plastic film dielectric and did not have a paper wick. This simple discussion of the basic capacitor geometry and construction methods serves as a basis for discussion of the capacitor failure mechanisms involved.

V. CAPACITOR FAILURE OBSERVATIONS AND DATA

A. Dielectric Degradation at Foil Edge

The failed PPSO capacitors were carefully disassembled and failed for the following reasons by approximate percentage:

5% defective fabrication
5% bulk dielectric failure
90% dielectric punch through at foil edge

The number of units that failed due to defective fabrication is above average. The bulk dielectric capacitor failures occurred around 10 thousand discharges and were usually due to defective dielectric material. The remainder and the majority of the capacitors failed at the foil edge. The failure mechanism is illustrated in Fig. 7 and consists of craters in the dielectric at many places along the foil edge that eventually eroded through the dieletric. Other observed damage, illustrated in Fig. 7, includes carbonization of voids in the dielectric, both in between the foils and at the foil edge.

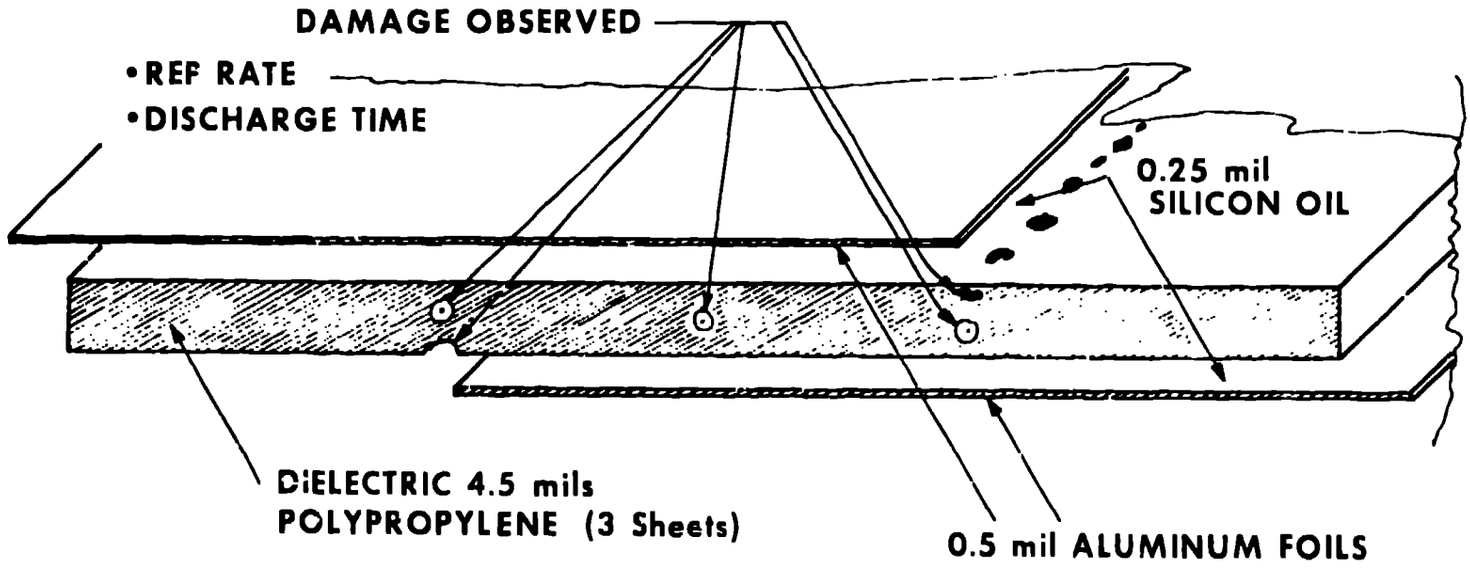

Fig. 7. Capacitor damage.

1. Position-Dependent Foil Edge Damage. Ninety percent of the foil edge damage occurred in the three outside wraps of the capacitor pack (Fig. 5) that is charged to the highest voltage with respect to ground or pack No. 1 (Fig. 6). The capacitor pack with the foil edge failures is on the end of the capacitor connected to the thyratron anode. The foil voltage on this end of the capacitor changes from the charge voltage ($\simeq$50 kV) to zero in approximately 40 ns and thus sees a large value of dV/dt.

The damage mechanism may have some relation to the transient current distribution during capacitor discharge. The capacitor pack (Fig. 5) can be used to illustrate the transient current flow. The discharge frequency is on the order of 10 MHz. The skin depth of the aluminum foil at 10 MHz is approximately equal to the foil thickness or 0.5 mil. Thus the charge stored in the interior of the capacitor cannot flow through the outer foils or the much thicker solder connections on top of the pack to the edge of the capacitor. The charge must therefore flow in a spiral path to the pack edge in a strip transmission line formed by two capacitor foils.

Transmission line effects may be responsible for dynamic voltage and thus electric field transients during discharge. The corona inception stress discussed previously suggests that during discharge, the dynamic electric field is approximately four times the average dc electric field. New capacitor pack connection designs that minimize current flow problems are being manufactured for test.

A second mechanism that may produce the location-dependent corona damage is the time rate of change of voltage (dV/dt) on the capacitor foil or pack with respect to ground. The capacitors tested were fabricated with an insulating phenolic case. Thus the outside few foils, especially in a low inductance circuit, are capacitively coupled to ground through stray capacitance. The stray capacitance is charged during the relatively slow (1 ms) charge of the test capacitor. Simultaneously, the high field at the edge of the foil can inject free charge into the margin region of the capacitor (Fig. 5). When the capacitor is discharged, (~100 ns) the free charge in the margin coupled to ground through stray capacitance is at the original capacitor potential while the foil is now grounded. This situation can conceivably produce extremely high local electrical fields between

the free charge in the margin and the foil edge. These high electric fields can also produce corona and dielectric degradation.

2. Scanning Electron Microscope/Ion Microprobe Observations.

Sections of the damaged dielectric were analyzed with a scanning electron microscope/ion microprobe system. This device allows identification of the materials in the sample at atomic levels. The microprobe results indicate that the foil edge damage shown in Fig. 8 as a black spot is an organic compound similar to the polypropylene dielectric. The black material is surrounded by a large amount of elementary hydrogen gas and a small amount of atomic oxygen, carbon, and silicon. The oxygen and silicon are probably the result of dissociation of the silicone oil impregnant. The picture of Fig. 9 reveals a small hydrogen gas bubble surrounding a black organic compound similar to polypropylene, all of which are inside a section of 1-mil polypropylene film. This damage also occurred at the foil edge. The ion microprobe analysis found no aluminum in areas of dielectric degradation.

Fig. 8. Ion microprobe sample.

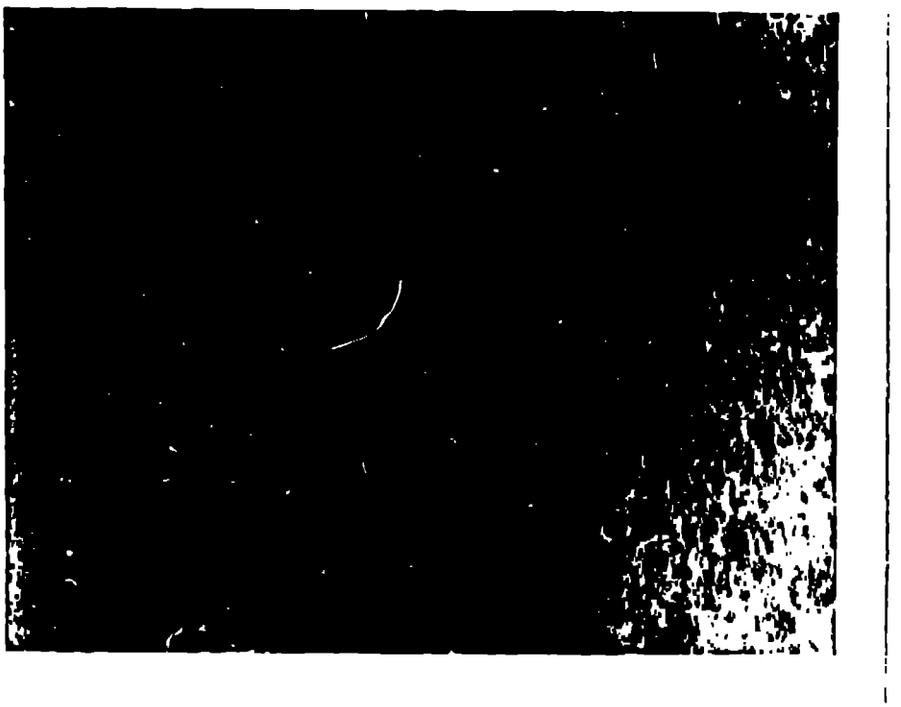

Fig. 9. Bulk dielectric damage.

3. Computer Aided Tomography Analysis. An x-ray, computer-aided tomography (CAT) system was used to scan the capacitor packs without disturbing the system. The diagram of Fig. 10 indicates that the CAT system was used to view 2-mm slices of the capacitor packs. A capacitor pack, foil-edge punch through is shown in Fig. 11 before failure of the entire capacitor but in the final stages in life. The density change observed with the CAT scan system indicates the presence of a void filled with gas, silicone oil, and assorted polypropylene derivatives.

This technique is ideal for nondestructive observation and evaluation of the capacitor physical integrity during test and evaluation.

B. Corona Inception

The capacitors were tested for dc integrity and corona before discharge testing. The dc corona inception level observed was slightly over twice the rated voltage or about 3000 V/mil in PPSO units. The dc high

Fig. 10. CAT scan of capacitor pack.

potential test, usually for several hours at rated dc voltage, was used to eliminate defective units.

When the test capacitors were discharged at a peak current of 1 kA in a 100-ns wide damped pulse, and a 1-kHz repetition rate, the corona inception stress level was observed to be only 875 V/mil. This implies that the dynamic electric fields within the capacitor are four times the dc electric field. The onset of corona during discharge is easily monitored by the facility diagnostic system as current trace blooming. In the test facility, the presence of corona is also detectable as very high frequency electromagnetic noise.

Corona inception is observed as an integrated effect. When operating the capacitor above the inception level, corona is not observed for some time, T_{CID}. If capacitor operation is halted after time, T_{CID}, and resumed in a few minutes, corona is immediately observed. If, however, capacitor operation is halted after corona observation for longer periods of time,

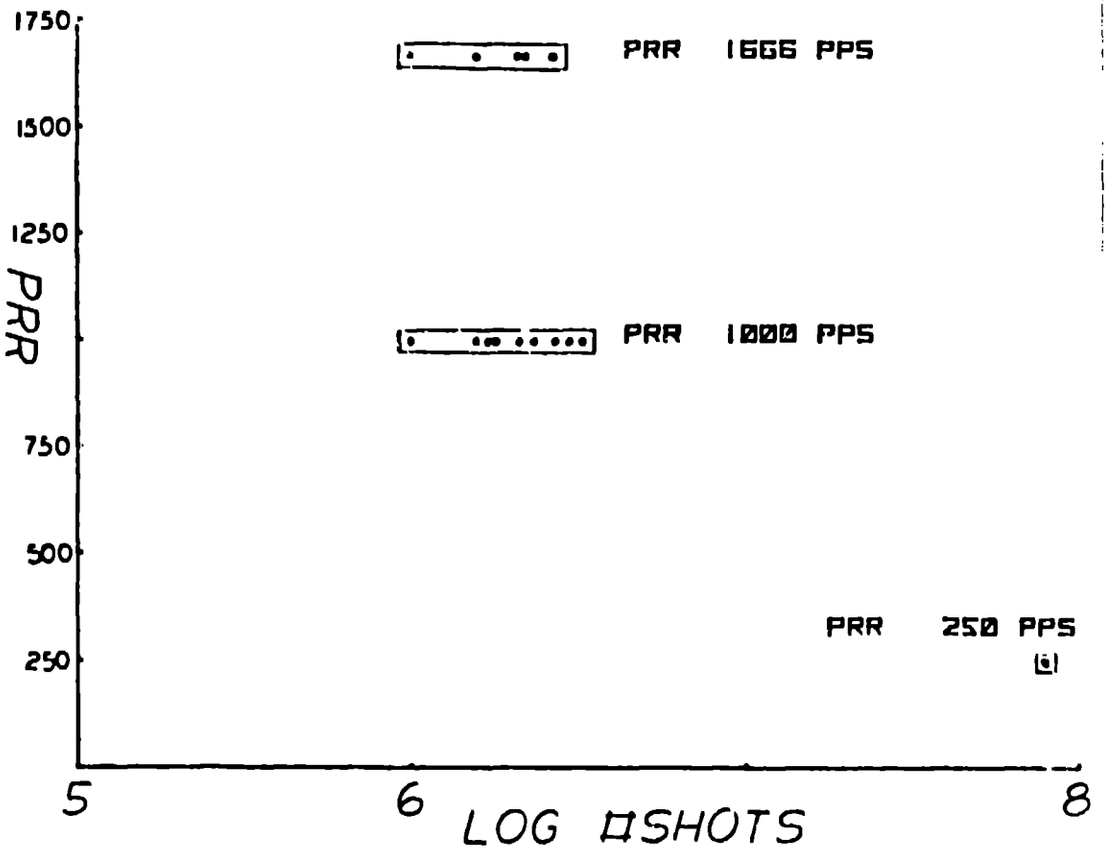

Fig. 11. PPSO capacitor life vs repetition rate.

say 24 hours, and then resumed there is a delay until corona is again observed, but the delay is less then the initial delay. This reduction in de' / time apparently continues over many start-stop-wait test cycles until the c na inception delay time, T_{CID}, approaches zero. The appearance of corona is assumed to be the result of dynamic electric fields much larger than the average dc stress levels. The corona damage observed occurs at the edge of the foil, and the high dynamic electric field apparently generates gas by dissociation of the impregnant and modification of the dielectric in regions of poor impregnation, bulk dielectric flaws, and high field. After sufficient gas has been generated, observable corona discharges. The renewable delay time or corona hysteresis effect with inactivity is presumably a result of the gas being redissolved in the impregnant. The event of zero corona onset delay after a period occurs when the local

impregnant is saturated with gas. After zero corona onset time delay, the internal gas pressure increases until the case explodes.

C. Corona Onset and Hysteresis with Repetition Frequency

The presence of corona was also found to be a function of and exhibited a hysteresis effect dependent on the discharge pulse repetition frequency (PRF). After the corona inception time delay, T_{CID}, the PRF was increased from 100 Hz, where no corona was observed, to 500-600 Hz where corona was observed on the current trace. In order to extinguish the corona, the PRF had to be reduced below 250-350 Hz. This can be tentatively explained again as a high dynamic electric field at the foil edge that oisassociates gas from the impregnant (silicone oil). If the e-folding (1/e) deionization time of the gas generated by the field at the foil edge is on the order of 1 ms, the residual ionization level due to one discharge pulse would be less than that required to affect the subsequent pulse ionization level if the subsequent pulse is spaced greater than 3-ms (330 Hz) or 3(1/e) times later. If this hypothesis is valid, discharge pulses spaced less than 3-ms apart would generate more ionization and gas than the previous pulse due to the initial ionization present. This hypothesis could also explain the observed hysteresis effect if the total amplitude of the ionization process increases in time for pulse spacing less than the e-folding (1/e) deionization time. In this case, the time required for the residual ionization level to decay below that required to influence the next pulse ionization process is longer, even though the e-folding time is the same.

D. Life vs Discharge Pulse Repetition Frequency

The life of PPSO capacitors is very dependent on the discharge PRF and is probably related to the corona dependence on PRF. A plot of capacitor life vs PRF (Fig. 11) indicates that the life of a capacitor increases drastically below approximately 500 Hz, the repetition frequency at which corona is observed.

Once a PPSO capacitor is operated in the corona regime, the life is limited to approximately 2.8×10^6 discharges regardless of PRF. This indicates that corona damage is accumulative. On the other hand, PPSO capacitors, when operated at lower dV/dt and lower dI/dt, have functioned for greater than 10^{10} shots in other parts of the test facility.

The Weibull distribution analysis of the failures indicates a single failure mechanism is responsible for failure, and the failure distribution is very narrow.

E. Capacitor Energy Dissipation

Initially, the dielectric loss and the equivalent series resistance of the capacitor was of major concern. However, the energy dissipated in the capacitors tested is so minimal that thermal effects have been neglected. For comparison, the temperature rise of a conventional Mylar paper capacitor is compared with that of a PFTE unit (Fig. 12). Both units were operated at a discharge PRF of 1 kHz, a peak current of approximately 1 kA in a 100-ns wide damped pulse. The test was halted after 42 minutes when the Mylar paper capacitor exploded due to the 65°C temperature compared to the 4.1°C temperature rise for the PFTE unit. The mica, PFTE, and PPSO capacitor units have a dissipative component so small that at present rms current levels up to 15 A, a maximum of only 10°C temperature rise, are observed.

VI. CONCLUSIONS

The performance evaluation of capacitors in the 100-ns, 1-kA, 1-kHz regime has led to the following observations:

- A high-quality, high-frequency diagnostic system is essential to observe transients within capacitors during discharge. The high-frequency CVRs and voltage probes developed for the system are most important diagnostic tools.
- Corona is the main cause of failure in PPSO capacitors and is detectable during discharge.
- The corona inception stress level during discharge is about 25% of the dc level and is dependent on rate of discharge, the position in capacitor, and the pulse repetition rate.
- Preliminary tests indicate that PTFE-silicone oil and mica paper (MP) capacitors have a longer life in the regime tested than the polypropylene-silicone oil units but with much lower energy density. This is attributed to the impregnation characteristics of PFTE units and fabrication methods of the MP units.

The Weibull distribution analysis of the failures indicates a single failure mechanism is responsible for failure, and the failure distribution is very narrow.

E. Capacitor Energy Dissipation

Initially, the dielectric loss and the equivalent series resistance of the capacitor was of major concern. However, the energy dissipated in the capacitors tested is so minimal that thermal effects have been neglected. For comparison, the temperature rise of a conventional Mylar paper capacitor is compared with that of a PFTE unit (Fig. 12). Both units were operated at a discharge PRF of 1 kHz, a peak current of approximately 1 kA in a 100-ns wide damped pulse. The test was halted after 42 minutes when the Mylar paper capacitor exploded due to the 65°C temperature compared to the 4.1°C temperature rise for the PFTE unit. The mica, PFTE, and PPSO capacitor units have a dissipative component so small that at present rms current levels up to 15 A, a maximum of only 10°C temperature rise, are observed.

VI. CONCLUSIONS

The performance evaluation of capacitors in the 100-ns, 1-kA, 1-kHz regime has led to the following observations:

- A high-quality, high-frequency diagnostic system is essential to observe transients within capacitors during discharge. The high-frequency CVRs and voltage probes developed for the system are most important diagnostic tools.
- Corona is the main cause of failure in PPSO capacitors and is detectable during discharge.
- The corona inception stress level during discharge is about 25% of the dc level and is dependent on rate of discharge and the pulse repetition rate.
- Preliminary tests indicate that PTFE-silicone oil and mica paper (MP) capacitors have a longer life in the regime tested than the polypropylene-silicone oil units but with much lower energy density. This is attributed to the impregnation characteristics of PFTE units and fabrication methods of the MP units.

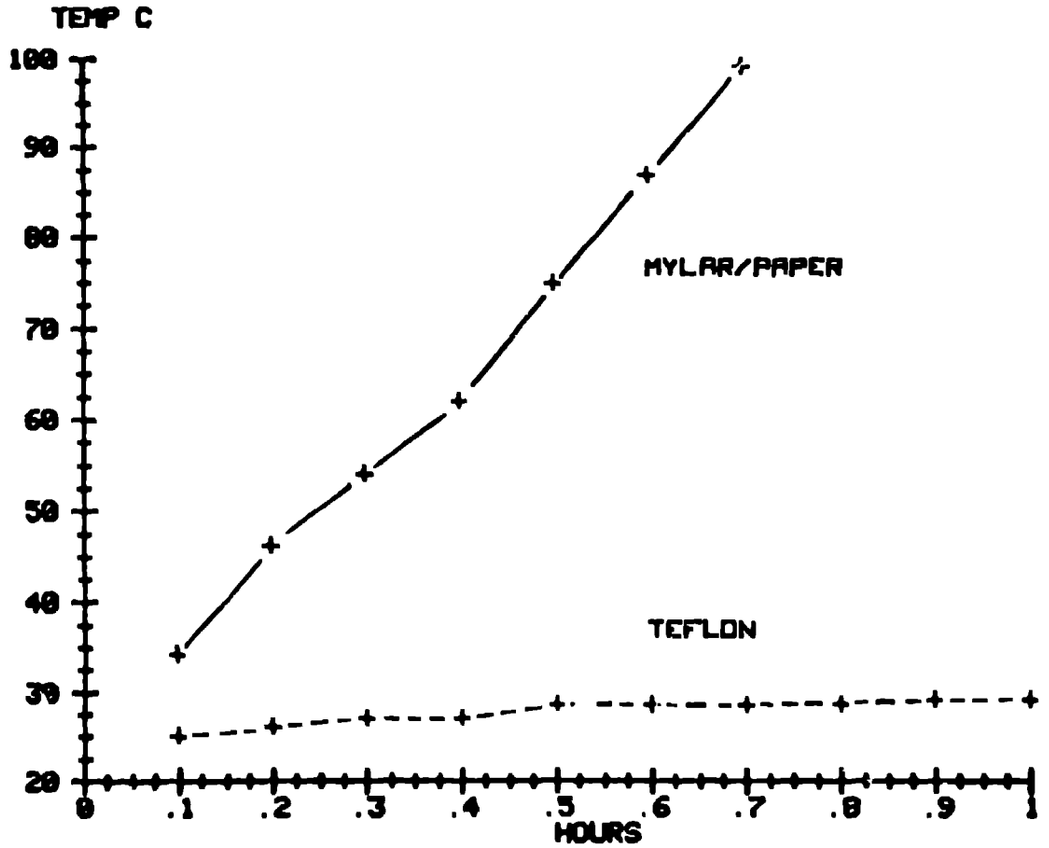

Fig. 12. Temperature rise of PFTE and MP capacitor.

- Capacitor power losses are negligible for units designed for this regime.
- Present fabrication techniques must be modified to accommodate the transient currents and voltages within the capacitor.

The PPSO capacitors were initially evaluated in detail because of the energy density potential, the relatively short lifetimes (3×10^6) that reduce the time required for evaluation, the availability and low cost, and the assumption that similar failure mechanisms would occur in the PFTE and MP units, but at longer life.

In the future the PFTE and MP units will be overstressed to decrease their lifetimes and thus determine their characteristic failure mechanisms. Additional CVR and high-voltage probe units are being designed to permit

higher frequency response at larger peak currents and voltages because of the large amount of data available with real-time diagnostic systems.

REFERENCES

1. R. D. Parker, "Technological Development of High Energy Density Capacitors," Hughes Aircraft Co., Report NASA CR124926, Culver City, CA, February 1976.

2. W. J. Sarjeant, "Energy Storage Capacitors," Los Alamos Scientific Laboratory Report LA-UR-79-1044, March 1979.